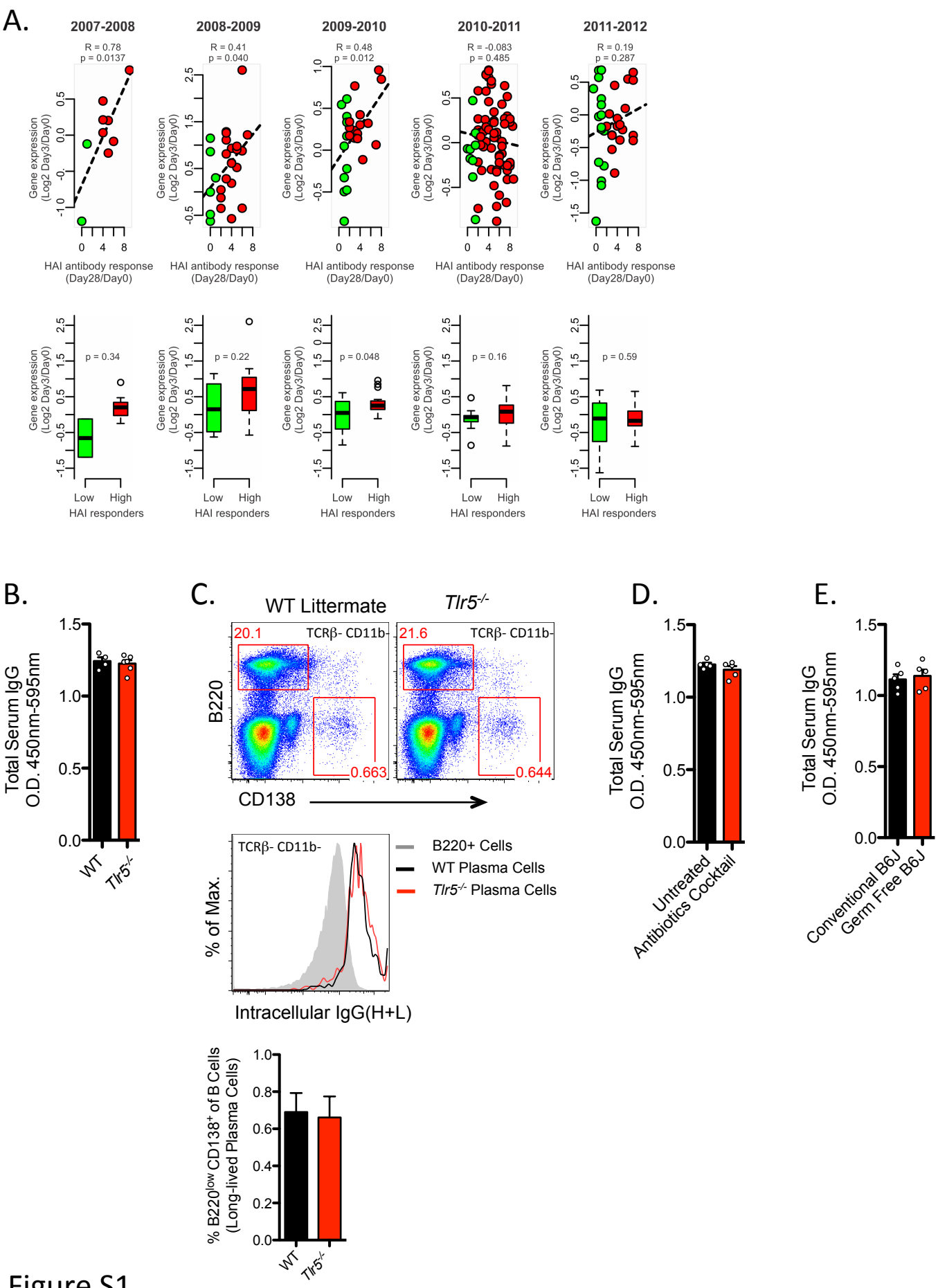
A.
2007-2008
2008-2009
2009-2010
2010-2011
2011-2012
R = 0.78
p = 0.0137
R = 0.41
p = 0.040
R = 0.48
p = 0.012
R = -0.083
p = 0.485
R = 0.19
p = 0.287
Gene expression (Log2 Day3/Day0)
HAI antibody response (Day28/Day0)
p = 0.34
p = 0.22
p = 0.048
p = 0.16
p = 0.59
Low
High
HAI responders
B.
Total Serum IgG O.D. 450nm-595nm
WT
Tlr5-/-
C.
WT Littermate
Tlr5-/-
20.1
21.6
TCRβ- CD11b-
B220
CD138
0.663
0.644
% of Max.
B220+ Cells
WT Plasma Cells
Tlr5-/- Plasma Cells
Intracellular IgG(H+L)
% B220low CD138+ of B Cells (Long-lived Plasma Cells)
D.
Untreated
Antibiotics Cocktail
E.
Conventional B6J
Germ Free B6J

Figure S1

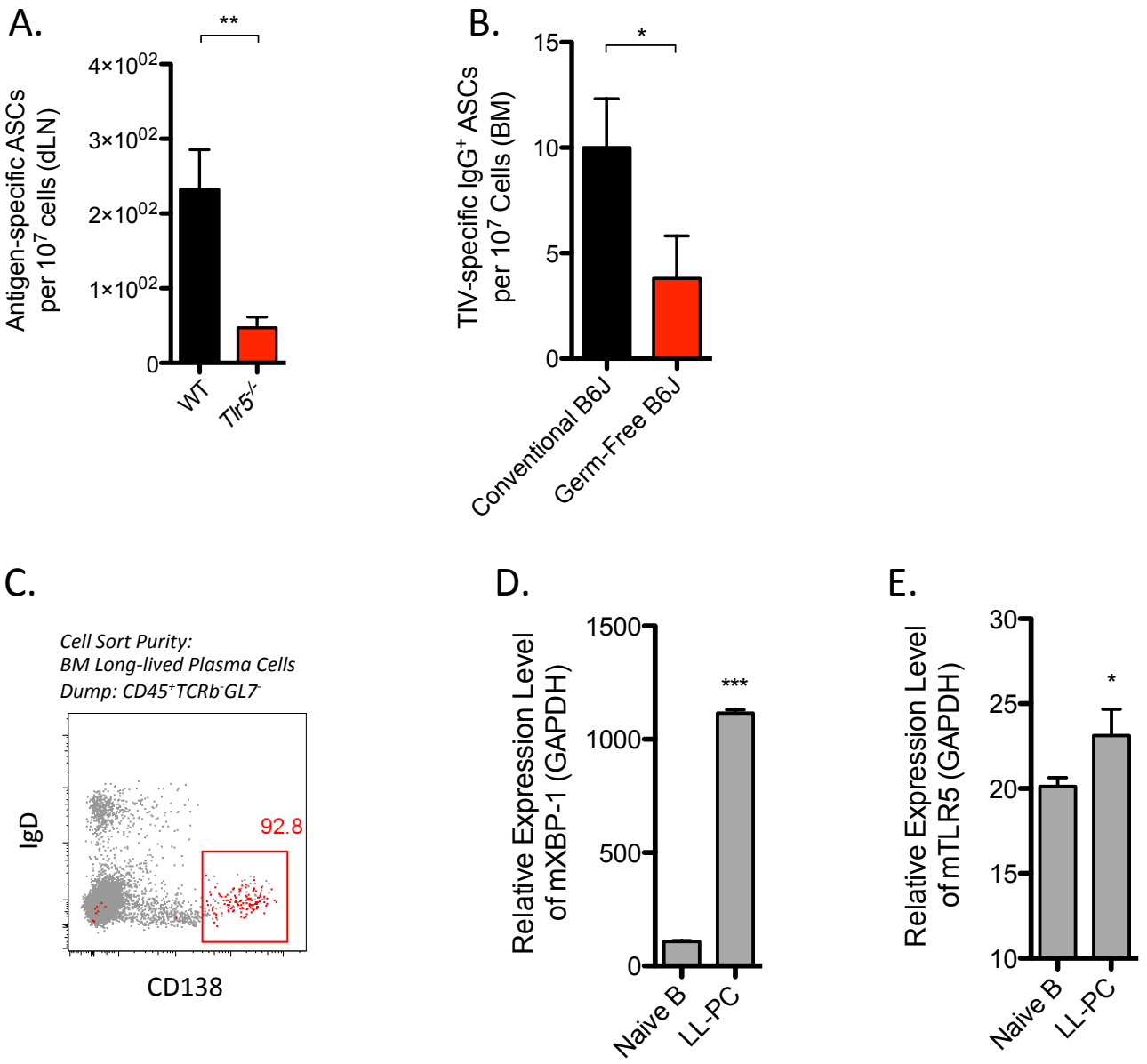
A.
**
Antigen-specific ASCs per 10^7 cells (dLN)
4×10^02
3×10^02
2×10^02
1×10^02
0
WT
Tlr5-/-
B.
*
TIV-specific IgG+ ASCs per 10^7 Cells (BM)
15
10
5
0
Conventional B6J
Germ-Free B6J
C.
Cell Sort Purity:
BM Long-lived Plasma Cells
Dump: CD45+TCRb-GL7-
IgD
92.8
CD138
D.
Relative Expression Level of mXBP-1 (GAPDH)
1500
1000
500
0
***
Naive B
LL-PC
E.
Relative Expression Level of mTLR5 (GAPDH)
30
25
20
15
10
*
Naive B
LL-PC

Figure S2

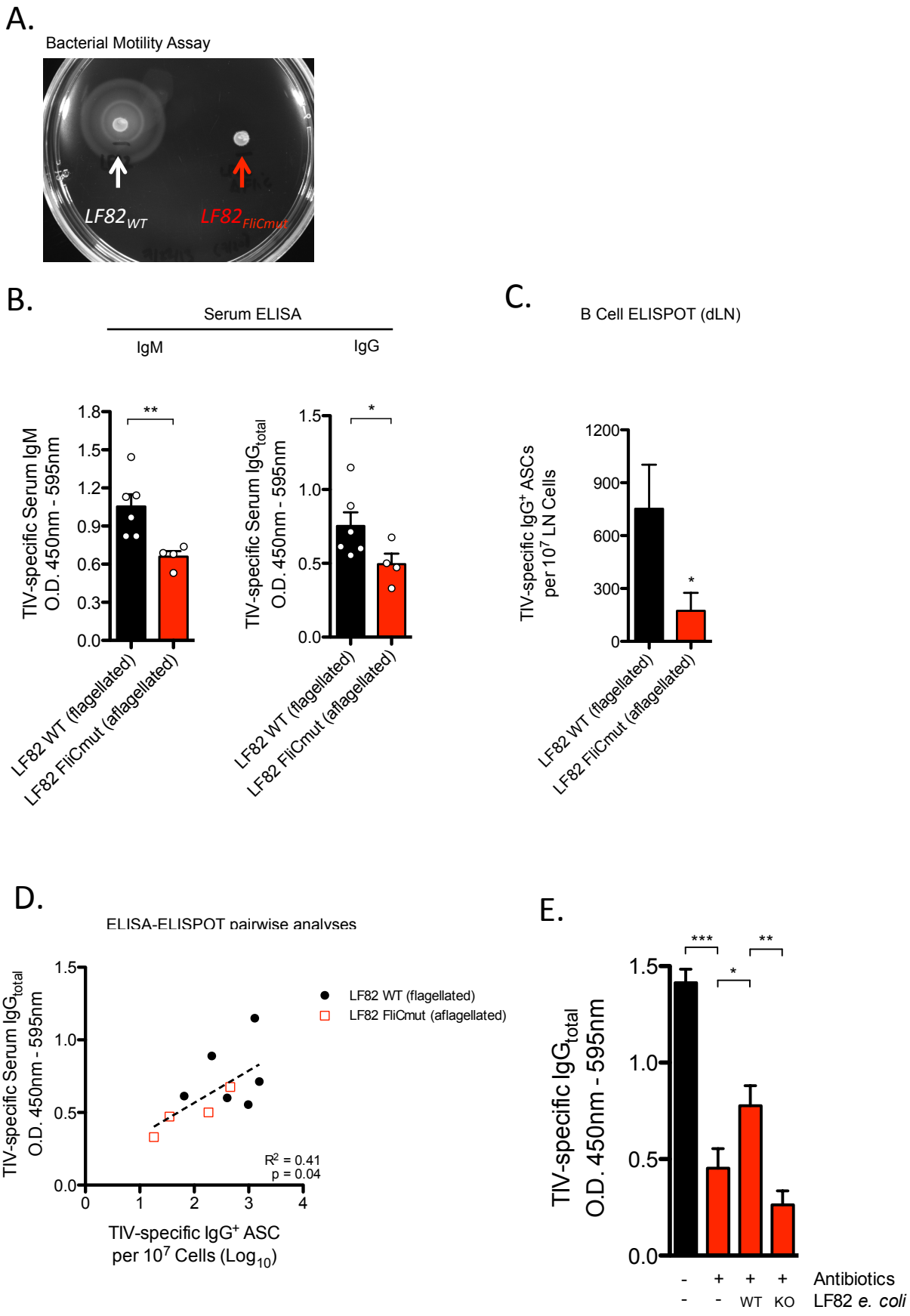
A.
Bacterial Motility Assay
LF82 WT
LF82 FliCmut
B.
Serum ELISA
IgM
IgG
TIV-specific Serum IgM O.D. 450nm - 595nm
TIV-specific Serum IgG total O.D. 450nm - 595nm
LF82 WT (flagellated)
LF82 FliCmut (aflagellated)
C.
B Cell ELISPOT (dLN)
TIV-specific IgG+ ASCs per 10^7 LN Cells
D.
ELISA-ELISPOT pairwise analyses
TIV-specific Serum IgG total O.D. 450nm - 595nm
TIV-specific IgG+ ASC per 10^7 Cells (Log10)
R2 = 0.41
p = 0.04
E.
TIV-specific IgG total O.D. 450nm - 595nm
Antibiotics
LF82 e. coli
WT
KO

Figure S3

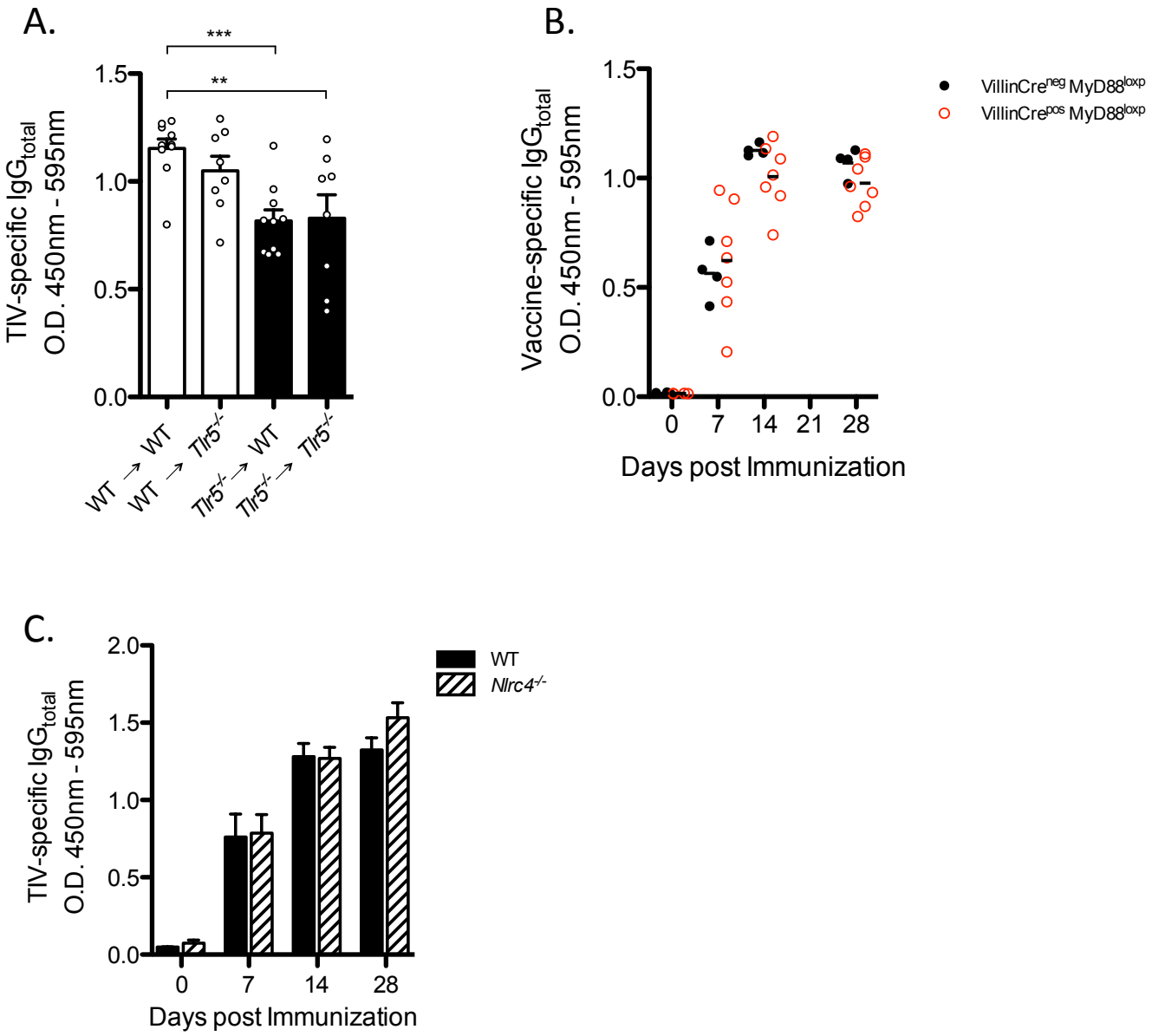
A.
***
**
TIV-specific IgG total
O.D. 450nm - 595nm
1.5
1.0
0.5
0.0
WT → WT
WT → Tlr5-/-
Tlr5-/- → WT
Tlr5-/- → Tlr5-/-
B.
Vaccine-specific IgG total
O.D. 450nm - 595nm
VillinCre neg MyD88 loxp
VillinCre pos MyD88 loxp
0
7
14
21
28
Days post Immunization
C.
TIV-specific IgG total
O.D. 450nm - 595nm
2.0
1.5
1.0
0.5
0.0
WT
Nlrc4-/-
0
7
14
28
Days post Immunization

Figure S4

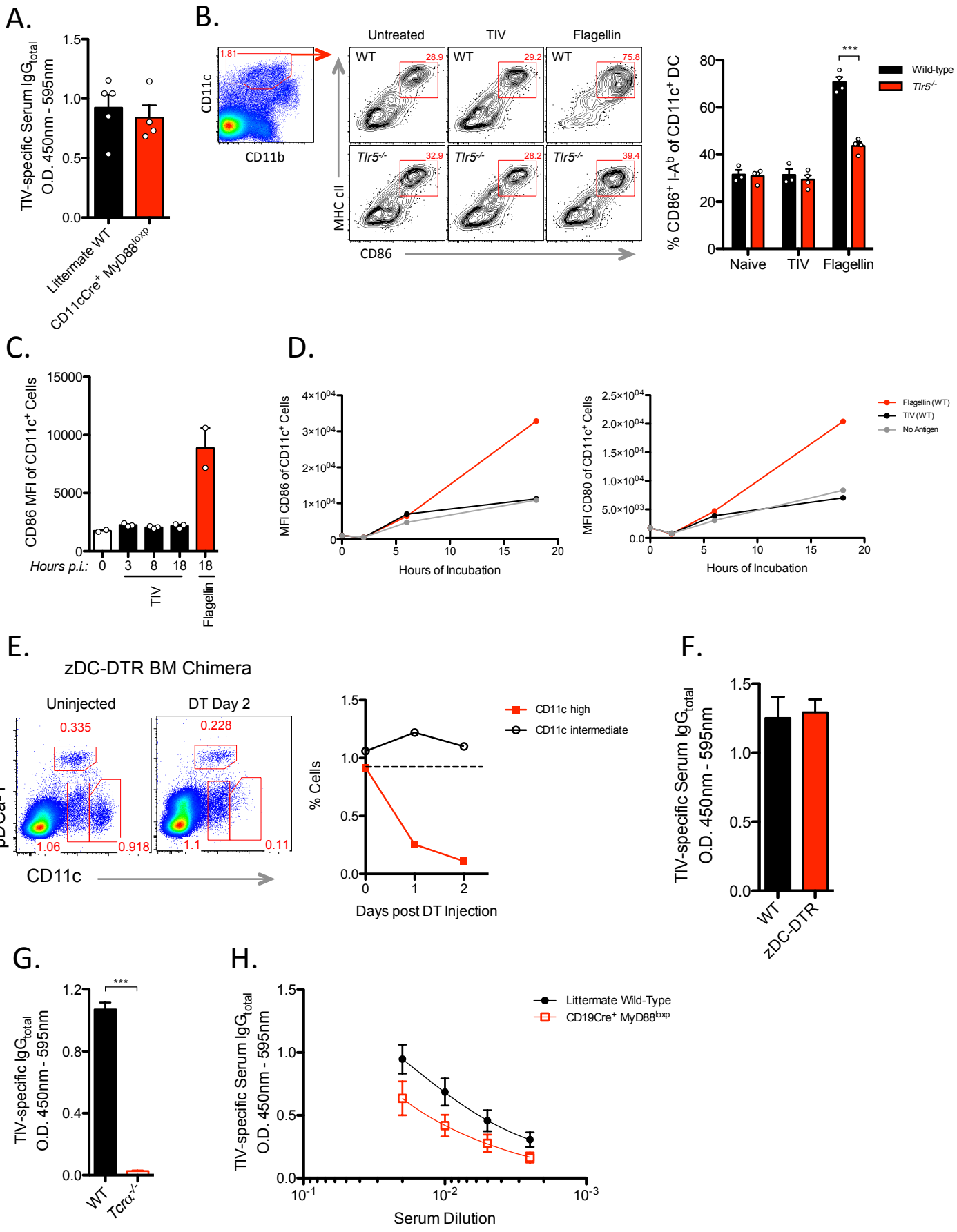
A.
TIV-specific Serum IgG_total O.D. 450nm - 595nm
Littermate WT
CD11cCre+ MyD88loxp
B.
Untreated
TIV
Flagellin
CD11c
CD11b
MHC cII
CD86
WT
Tlr5-/-
% CD86+ I-Ab of CD11c+ DC
Wild-type
Tlr5-/-
Naive
TIV
Flagellin
C.
CD86 MFI of CD11c+ Cells
Hours p.i.:
TIV
Flagellin
D.
MFI CD86 of CD11c+ Cells
MFI CD80 of CD11c+ Cells
Hours of Incubation
Flagellin (WT)
TIV (WT)
No Antigen
E.
zDC-DTR BM Chimera
Uninjected
DT Day 2
pDCa-1
CD11c
% Cells
Days post DT Injection
CD11c high
CD11c intermediate
F.
TIV-specific Serum IgG_total O.D. 450nm - 595nm
WT
zDC-DTR
G.
TIV-specific IgG_total O.D. 450nm - 595nm
WT
Tcrα-/-
H.
TIV-specific Serum IgG_total O.D. 450nm - 595nm
Littermate Wild-Type
CD19Cre+ MyD88loxp
Serum Dilution

Figure S5

A.

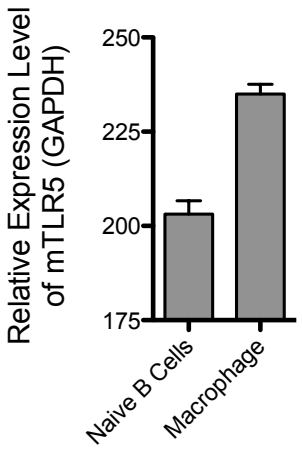

B.

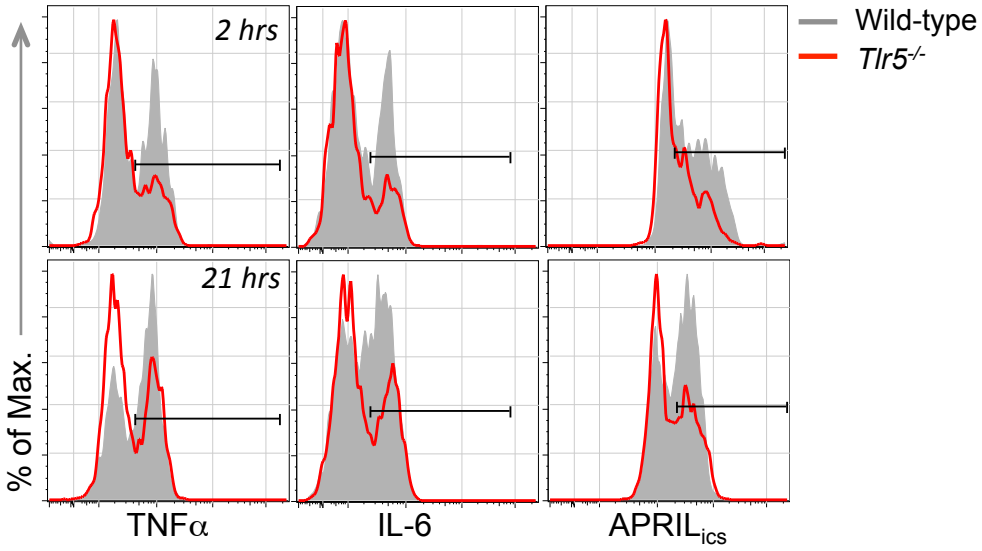

C.

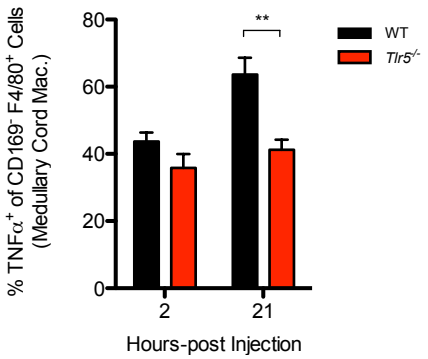

D.

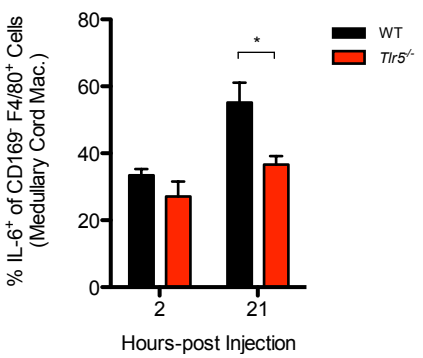

E.

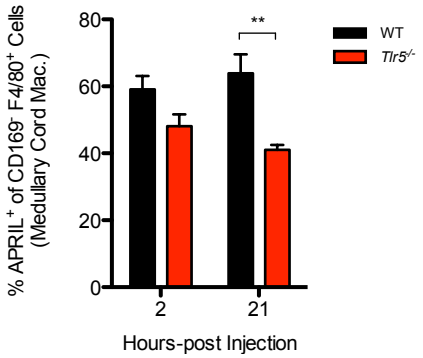

Figure S6

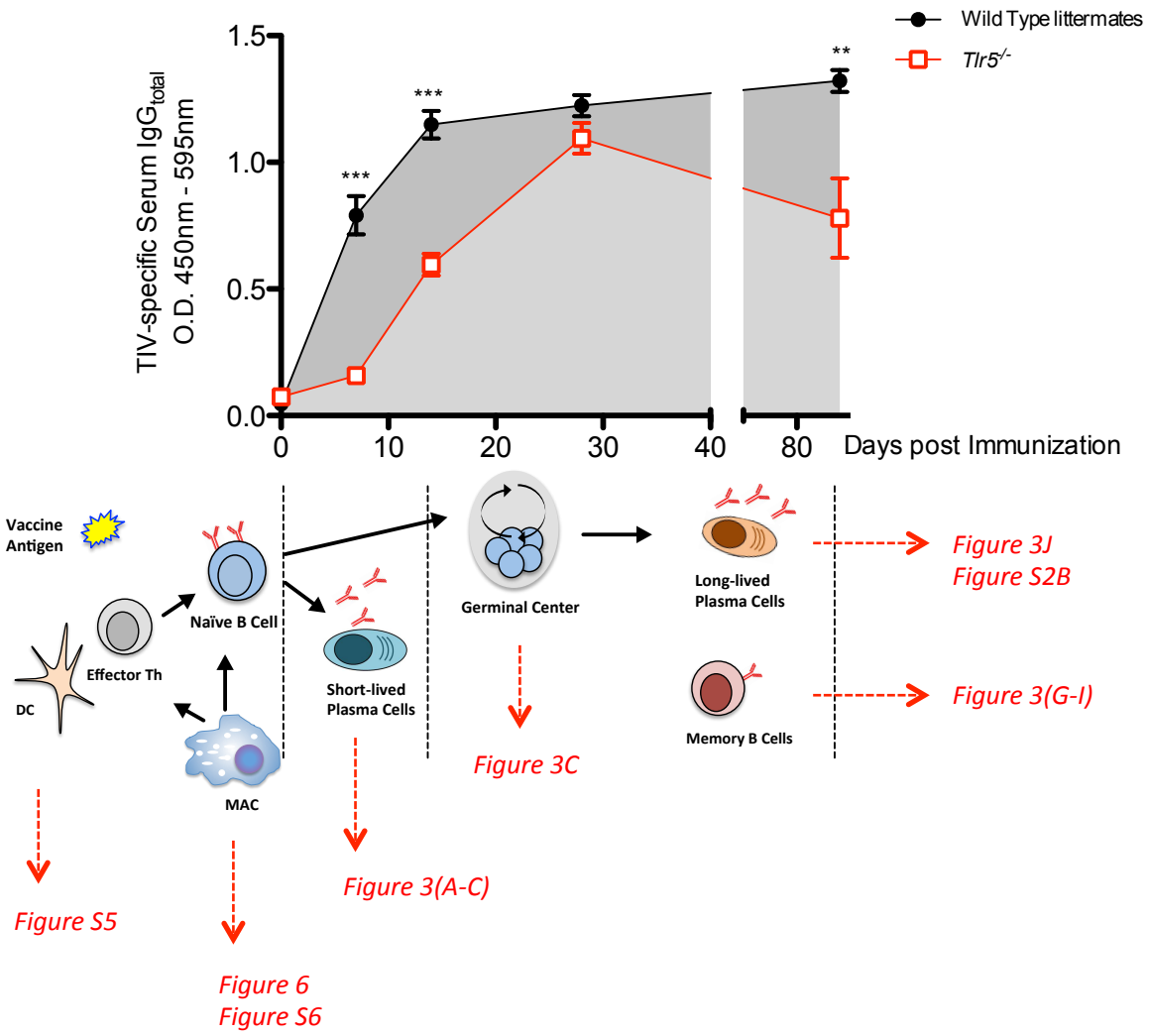
Wild Type littermates
Tlr5-/-
TIV-specific Serum IgGtotal
O.D. 450nm - 595nm
1.5
1.0
0.5
0.0
***
***
**
0
10
20
30
40
80
Days post Immunization
Vaccine Antigen
Naïve B Cell
Effector Th
DC
MAC
Short-lived Plasma Cells
Germinal Center
Long-lived Plasma Cells
Memory B Cells
Figure 3J
Figure S2B
Figure 3(G-I)
Figure 3C
Figure 3(A-C)
Figure S5
Figure 6
Figure S6

Figure S7

SUPPLEMENTAL FIGURE LEGENDS

Figure S1, related to Figure 1. Induction of TLR5 expression at day 3 post-vaccination correlates with antibody responses in humans, but *Tlr5*$^{-/-}$, antibiotic-treated, and germ-free mice do not exhibit pre-existing defects in humoral immunity.

(A) Based on microarray data obtained from clinical studies previously conducted by our group (Nakaya et al., 2011. *Nat. Immunol*. & manuscript in preparation), we compared the TLR5 expression patterns from the PBMCs of subjected vaccinated with TIV with the magnitude of hemagglutination-inhibition (HAI) antibody titers in response to vaccination. The scatter plots represent the baseline-normalized TLR5 expression at day 3 (y axis) and the antibody HAI responses at day 28 (x axis) in 5 consecutive influenza seasons (2007 to 2011). TIV vaccinees considered high responders (≥ 4-fold increase and ≥ 1:40 titers at day 28 compared to baseline in at least one of the 3 influenza strains in the vaccine) were shown in red and low responders in green. The box plots at the bottom represent the student's t-test between low (green) and high (red) antibody TIV responders. (B-E) Total serum IgG antibody levels in naïve (B) littermate WT B6 or TLR5-/- mice, (D) untreated or antibiotic-treated WT B6 mice, or (E) conventional or germ-free B6 mice. Raw O.D. values shown were obtained using serum diluted by a factor of 1:2000. Data are represented as means ± SEM. Relative frequencies of long-lived plasma cells in the bone marrow were measured by FACS (C). Representative dot plots of lineage negative (TCRb-CD11b-) bone marrow cells from littermate WT and *Tlr5*$^{-/-}$ mice are shown and the frequencies of plasma cells (B220low CD138+) are represented in the

graph shown. Histogram of intracellular IgG levels within B220low CD138+ gated plasma cells are shown in comparison to B220+ B cells.

Figure S2, related Figure 2. TIV-induced short-lived plasma cells in the draining LN and long-lived plasma cells in the bone marrow are reduced in *Tlr5*$^{-/-}$ and germ-free mice, and TLR5 is upregulated in plasma cells of the bone marrow

Frequency of TIV-specific IgG+ antibody secreting cells in the dLN of Tlr5-/- mice on day 7-post vaccination (A) and in the bone marrow of germ-free mice on day 28-post vaccination (B). Data are represented as the means ± SEM. (C) Dot plot representative of gating scheme and efficiency of flow-sorted plasma cells from the bone marrow. Frequency shown is the percent purity of isolated plasma cells.

(D) XBP-1 mRNA levels and (E) TLR5 mRNA levels in naive B cells from LNs and LL-PCs from the bone marrow analyzed by quantitative real-time PCR. Data represent means (normalized to GAPDH) in arbitrary units ± SEM.

Figure S3, related to Figure 3. Colonization or inoculation of flagellated bacteria in the gut enhances antibody response to TIV.

(A) Bacterial motility assay using the flagellated *E. coli* strain LF82 and its isogenic aflagellated mutant strain, LF82FliCmut. Photograph shown depicts radial cell dispersion of flagellated bacteria from a single inoculation point in a LB agar plate (6 hours).

(B) TIV-specific IgM and IgG levels in the serum of germ-free B6 mice colonized with either LF82 or LF82FliCmut bacteria (Day 7-post vaccination).

(C) Frequency of TIV-specific ASCs in the draining LN (Day 7-post vaccination)

(D) Pairwise analysis between the levels of TIV-specific serum IgG antibodies (B) and corresponding frequencies of TIV-specific ASCs (C).

(E) TIV-specific IgG levels in the serum of antibiotic-treated and untreated mice that received four daily oral gavages with LF82 or LF82FliCmut bacteria (Day 7-post vaccination). Data shown are means ± SEM.

Figure S4, related to Figure 4. TIV induced antibody responses do not require TLR5 or MyD88 signaling in non-hematopoietic and gut epithelial cells, respectively, and do not require signaling via the NLRC4-inflammasome pathway

TIV-specific IgG levels in (A) bone marrow chimeric mice (donor genotype → recipient genotype) (Day 22-post vaccination), (B) Villin-Cre+ MyD88loxp or MyD88loxp mice, (C) Wild-type or *Nlrc4*$^{-/-}$ mice. Raw O.D. values were obtained using serum diluted at (A) 1:100, (B, C) 1:200, and represented as the means ± SEM.

Figure S5, related to Figure 5. Dendritic cells are not directly activated by TIV and are dispensable during TIV-induced antibody response, but T cells are required and partial dependency on MyD88 signaling in B cells is observed

(A) TIV-specific IgG levels in CD11c-Cre+ MyD88loxp or littermate Cre- MyD88loxp mice (day 7-post vaccination)

(B) Representative dot plots of TCRb-B220- gated cells depicting cell frequency and expression levels of CD86 and MHC class II molecule, I-Ab within CD11c+ gated population of cells. Shown on the right is a graphical representation of the data as the means ± SEM.

(C) Level of CD86 expression in CD11c+ DCs in the dLN at the indicated time points following injection with TIV or flagellin.

(D) Levels of CD86 and CD80 expression on splenic DCs stimulated *in vitro* with flagellin (800 ng/mL) or TIV (1:16 dilution). Data are expressed as means ± SEM.

(E) Efficiency of DT-mediated depletion of conventional DCs in zDC-DTR bone marrow chimeric mice. Representative dot plots of LNs following DT administration are shown. Relative frequencies of DCs are graphically represented.

(F) TIV-specific IgG levels in zDC-DTR chimeric mice (day 14-post vaccination). Raw O.D. values were obtained using serum diluted at 1:200.

(G) TIV-specific IgG levels in *Tcrα*$^{-/-}$ (day 14-post vaccination). Shown O.D. values were obtained using serum diluted at 1:200 and represented as the means ± SEM.

(H) TIV-specific IgG levels in CD19Cre+ MyD88loxp or littermate Cre- MyD88loxp mice (day 7-post vaccination). Shown O.D. values obtained at the indicated titration of serum samples and represented as the the means ± SEM.

Figure S6, related to Figure 6. Expression of TLR5 in LN macrophages and TLR5-dependent inflammatory cytokine production by medullary cord macrophages in response to flagellin *in vivo*

(A) TLR5 mRNA levels in LN macrophages in comparison with naïve B cells were analyzed by qRT-PCR. Data represent mean levels of TLR5 mRNA (normalized to GAPDH) and expressed as arbitrary units ± SEM.

(B) Representative histograms depicting levels of intracellular cytokine production in medullary cord macrophages isolated from the dLN of mice injected with flagellin (21 hours-post injection).

(C-E) Relative frequencies of TNFα, IL-6, or APRIL producing macrophages are shown as the means ± SEM.

Figure S7, related to Figure 7. Mechanism of TLR5-mediated Induction of Humoral Immune Response to TIV

Graph of the kinetics of the primary IgG response to TIV was shown in (Figure 3D). Below, different phases of the humoral immune response as well as the preceding components of the innate immune system are depicted. Data corresponding to each phase of the immune response are referenced.

SUPPLEMENTAL EXPERIMENTAL PROCEDURES

Mice and Immunizations

C57BL/6 (Charles River Laboratory, Jackson Laboratory), *Nlrc4*$^{-/-}$, *Tcrα*$^{-/-}$ (Jackson Laboratory), *Villin*^{Cre}*Myd88*^{loxp}, *Cd11c*^{Cre}*Myd88*^{loxp}, *Cd19*^{Cre}*Myd88*^{loxp} mice were maintained in specific-pathogen-free conditions at the Emory Vaccine Center vivarium in accordance with all animal protocols reviewed and approved by the Institute Animal Care and Use Committee of Emory University. Germ-free C57BL/6 mice were maintained at the National Gnotobiotic Rodent Resource Center of the University of North Carolina using standardized protocols (Gulati et al., 2012). LysM^{Cre} Myd88^{loxp} were maintained at the University of Texas Southwestern Medical Center. Mice were immunized subcutaneously with the following vaccines: TIV (Fluvirin, Novartis; Fluarix, GlaxoSmithKline Biologicals), IPOL (Sanofi Pasteur SA), Tdap (Adacel, Sanofi Pasteur SA), Recombivax HB (Merck) were used at 1:5 dilution of adult dose per mouse; HIVgp140 envelope adsorbed in alum (1% Aldrylgel Al(OH)3) was used at 10 mg per mouse; YF-17D was used at 2x10^6 pfu per mouse. Flagellin was administered at 20 μg per mouse alone or 10 μg per mouse in combination with TIV.

TLR5-NFkB HEK Reporter Assay

HEK293 cell line was co-transfected with a plasmid containing the human TLR5 gene and the NF-kB reporter plasmid, pNiFty2-SEAP (Invivogen). Stably transfected cells were cultured with a panel of TLR agonists, virus, or vaccines as follows: Flagellin (1 mg/mL), LPS (100 ng/mL), Poly(I:C) (HMW) (100 ng/mL), and Resiquimod R848 (10 mg/mL) (Invivogen), Influenza virus (A/Brisbane/59/2007) (1 MOI), TIV (Fluvirin,

Novartis) and the live-attenuated influenza vaccine (Flumist, Medimmune) (1:10 dilution). Levels of SEAP in the culture supernatant were determined at 20 hours of incubation at 37^{o}C using QUANTI-Blue detection medium according to manufacturer's protocol (Invivogen).

ELISA

Nunc Maxisorp plates were coated with TIV (1:40 dilution), IPOL (1:40), Tdap (1:30), Recombivax HB (1:20), HIVenv (1.5 mg/mL), YF-17D 10x10^{6} pfu/mL), or goat anti-mouse IgG (1 μg/mL) (Southern Biotech) and incubated overnight at 4^{o}C. Plates were washed 3 times with 0.5% Tween-20/PBS and blocked with 200 μl of 4% non-fat dry milk (Biorad). Mouse serum samples were serially diluted in 0.1% non-fat dry milk in 0.5% Tween-20/PBS and incubated on blocked plates. Antigen-specific serum antibodies were detected using horseradish peroxidase (HRP) conjugated antibodies (anti-mouse IgG, anti-mouse IgG1, anti-mouse IgG2c, and anti-mouse IgM) (Southern Biotech) at 1:5000 dilution in 0.1% non-fat dry milk in 0.5% Tween-20/PBS. Incubation of serum samples or antibodies was conducted at room temperature. HRP activity was detected using 100 μL of tetramethylbenzidine (TMB) substrate (BD Biosciences) and stopped using 50 μL 2N H_2SO_4 per well. Developed plates were recorded using BioRad spectrophotometer at 450 nm with correction at 595 nm by subtraction. IL-6 ELISA was conducted according to manufacturer's protocol (BD).

B Cell ELISPOT Assay

Multiscreen-HA ELISPOT plates (Millipore) were coated TIV (1:40 dilution in PBS) and incubated for 2 hours at 37^{o}C. Coated plates were washed with PBS and blocked in 200 μL per well with supplemented RPMI culture media (10% FBS) for 2 hours at room temperature. Cell suspensions prepared from either the draining lymph nodes or bone marrow were serially diluted from known cell concentrations in supplemented RPMI culture media and transferred to the blocked ELISPOT plates. Following 12-18 hour incubation at 37^{o}C, plates were washed and treated with biotinylated goat anti-mouse total IgG (Southern Biotech) in 0.5% Tween-20/1% FBS/PBS for 1.5 hours. Plates were then washed and treated with streptavidin alkaline phosphatase (Vector Labs) at a 1:500 dilution in 0.5% Tween-20/1% FBS/PBS for 1 hour. All wash steps were conducted using 0.5% Tween-20/PBS. Incubations were conducted at room temperature unless noted otherwise. Presence of antigen-specific antibodies was detected using NBT/BCIP colorimetric substrate (eBioscience) at 80 μL per well. Reaction was terminated once the formation of discrete purple-colored spots was detected. Spots were counted using the CTL ImmunoSpot ELISPOT software.

Generation of Bone Marrow Chimera

Bone marrow cells were obtained from the femur and tibia of either *Tlr5*$^{-/-}$ or littermate wild-type mice. Irradiated (850r) recipient mice were injected with approximately 4x10^{6} bone marrow cells per mouse. Hematopoietic cell compartments derived from respective bone marrow donor types were allowed to reconstitute recipient mice for five weeks.

Bacterial DNA Quantification and Compositional Analyses of Gut Microbiota

Bacterial genomic DNA was extracted from stool samples using either QIAamp DNA stool mini kit (Qiagen) for quantitative analyses or PowerSoil-htp kit from MoBio Laboratories (Carlsbad, California, USA) for DNA sequence-based compositional analyses. qPCR was performed using SYBR® Green I dye chemistry (Qiagen).
For compositional analyses, 16sRNA gene was amplified using primer pairs containing unique 12-base barcodes to tag PCR products from respective samples as previously described (Chassaing et al., 2013; Hamady et al., 2008). Briefly, PCR products were sequenced using a Roche 454 Titanium pyrosequencer and analyzed using Quantitative Insights into Microbial Ecology (QIIME) (Caporaso et al., 2010). Further details are available in Supplemental Information.

Gene Expression Analyses

Total RNA from sorted plasmablast/short-lived PCs or naïve B cells was extracted using RNeasy Minikit (Qiagen). cDNA was obtained using Superscript III (Invitrogen). Quantitative RT-PCR was conducted using QuantiFast SYBR Green PCR kit (Qiagen) and Bio-rad iQ5 cycler according to manufacturer's protocols. Primers specific for TLR5 and GAPDH were previously described (Edwards et al., 2003).

Dendritic Cell Stimulation in vitro

Cell suspensions prepared from wild-type spleen samples were plated at $1x10^6$ cells per well in a 96-well plate. Dilutions of either TIV or purified flagellin were mixed with the plated cells (in triplicates) and incubated at 37^oC. At various time points of incubation,

cells were transferred from culture for staining by a panel of fluorescently labeled antibodies as described above to examine status of DC activation.

Bacterial DNA Quantification and Compositional Analyses of Gut Microbiota

Bacterial genomic DNA was extracted from stool samples using either QIAamp DNA stool mini kit (Qiagen) for quantitative analyses or PowerSoil-htp kit from MoBio Laboratories for DNA sequence-based compositional analyses. For quantification of bacterial load, qPCR was performed using SYBR® Green I dye chemistry and 7300 Real-Time PCR Systems and Software (Applied Biosystems). Each 50 µl reaction contained 10-30 ng of fecal DNA, 25 µl of 2x SYBR® Green PCR Master Mix (Applied Biosystems), 40 nM of the bacteria-specific primer 8F (5'-AGAGTTTGATCCTGGCTCAG-3'), and 40 nM of the universal primer 338R (5'-CTGCTGCCTCCCGTAGGAGT-3') (Invitrogen). Standard curves were prepared from serial dilution of *E. coli*-25 genomic DNA extracted in the same manner as above and all samples were run in duplicate or triplicates. Cycling conditions were 50°C for 2 min., followed by 95°C for 10 min, followed by 40 cycles of 95°C for 30 sec. and 56°C for 1 min., with a final melting curve period of 95°C for 15 sec., 60°C for 30 sec., and another 15 sec. at 95°C.

For compositional analyses, 16sRNA gene was amplified using primer pairs containing unique 12-base barcodes to tag PCR products from respective samples as previously described (Chassaing et al., 2013; Hamady et al., 2008). Tagged and pooled PCR products were sequenced using a Roche 454 Titanium pyrosequencer. Sequence results were compiled and analyzed using the open source software package, Quantitative

Insights into Microbial Ecology (QIIME) (Caporaso et al., 2010). The 16S gene sequences were aligned and clustered using UCLUST (Edgar, 2010) with a pair-wise identity threshold of 97%. Clustered sequences were assigned operational taxonomic units (OTUs) and a single representative sequence for each OTU was aligned using PyNAST to enable taxonomic classification and generation of phylogenetic trees for subsequent analyses. Phylogenetic data were used to compute distances or levels of dissimilarity between microbial communities using Unifrac (Lozupone and Knight, 2005). QIIME was used to generate a 2-dimensional principal coordinate analysis plots to represent the unweighted UniFrac metrics.

Gene Expression Analyses

Total RNA from sorted long-lived plasma cells in the bone marrow, naïve B cells or macrophages from the LN was extracted using RNeasy Minikit (Qiagen). cDNA was obtained using Superscript III (Invitrogen). Quantitative RT-PCR was conducted using QuantiFast SYBR Green PCR kit (Qiagen) and Bio-rad iQ5 cycler according to manufacturer's protocols. Cells were flow-sorted based on CD138+IgD- expression for LL-PCs and CD19+IgD+ expression for naïve B cells in CD45+CD11b-TCRb- gated population of cells. Naïve B cells and macrophages were flow-sorted based on CD45+TCRb-CD11b-CD19+IgD+ and CD45+TCRb-CD19-F4/80+ gated population of cells, respectively.

Bacterial Motility Assay

Flagellated *E. coli* strain, LF82 (Darfeuille-Michaud et al., 2004), and its isogenic aflagellated mutant strain, LF82FliCmut (Barnich et al., 2003), were inoculated into LB plates (0.3% agar) and dispersion of cells were assessed following 6 hours of incubation at 37^{o}C.

Bacterial Colonization of Germ-free and Antibiotic-treated Mice

Mice treated with the cocktail of broad-spectrum antibiotics (for 4 consecutive weeks) or untreated were orally gavageed with *E. coli* LF82 or LF82flic-/- once daily for 4 days and vaccinated with TIV following the last day of gavage. (C) Germ-free B6 mice were colonized with either LF82 or LF82flic-/- via oral gavage in separate micro-isolators and vaccinated with TIV 3 days following bacterial gavage. On Day 7-post vaccination, (B, C) TIV-specific IgG and (C) IgM levels in the serum were measured using ELISA as previously describe. (D) Frequency of antigen-specific ASCs in the draining LN was assessed by B cell ELISPOT asasy. (E) Pairwise analysis was conducted using the levels of TIV-specific serum IgG antibodies measured by ELISA corresponding to the frequency of TIV-specific ASCs in the dLN.

zDC-DTR Bone Marrow Chimera and Dendritic Cell Depletion

Bone marrow chimeric mice were generated using donor cells from zDC-DTR mice and congenic recipient mice. Efficiency of DT-mediated depletion of conventional DCs in reconstituted mice is shown in (C). These zDC-DTR chimeric mice were vaccinated with TIV following DT administration and TIV-specific IgG antibody response was

determined by serum ELISA. (D) Data of raw O.D. values were obtained using serum diluted at 1:200.

Flow Cytometry

Cell suspensions from dLN or bone marrow were stained with the following fluorochrome-labeled mAbs in the presence of blocking mAb, 2.4G2 (anti-FcγRIII/I): CD19 (6DS), CD138 (281-2), TCRb (H57-597), Ly-6C (HK1.4), CD11c (N418), CD256 (APRIL, A3D8), pDCa-1 (927) from Biolegend; B220 (RA3-6B2), GL-7 (GL-7), F4/80 (BM8), CD169 (SER-4), IL-6 (MP5-20F3), TNFα (MP6-XT22) from eBioscience; CD45 (30-F11), CD11b (M1/70), CD86 (GL1), I-Ab (25-9-17) from BD Pharmingen; IgG_{H+L} from Invitrogen. To distinguish live/dead cells, some samples were stained with Alexa Fluor 430 (Invitrogen) prior to staining with mAbs. In experiments examining macrophages, tissue samples were collagenase-digested prior to staining. Sample data were acquired on LSRII Flow Cytometers (BD Biosciences) and analyzed using Flowjo (Treestar).

Statistics

Statistical significance was determined by t-test using Prism software (GraphPad). Probability values of $p \leq 0.05$ were considered significant and denoted by *. Where indicated, ** denotes $p \leq 0.005$ and *** $p \leq 0.0005$. A 'nearest-shrunken centroid' classification approach was performed to detect OTUs that were particularly representative of each experimental group (Tibshirani et al., 2002). The amount of

shrinkage was set to minimize the misclassification error. These analyses were performed using the Prediction Analysis for Microarrays (PAM) package within R software.

SUPPLEMENTAL REFERENCES

Barnich, N., Boudeau, J., Claret, L., and Darfeuille-Michaud, A. (2003). Regulatory and functional co-operation of flagella and type 1 pili in adhesive and invasive abilities of AIEC strain LF82 isolated from a patient with Crohn's disease. Molecular microbiology *48*, 781-794.

Caporaso, J.G., Kuczynski, J., Stombaugh, J., Bittinger, K., Bushman, F.D., Costello, E.K., Fierer, N., Pena, A.G., Goodrich, J.K., Gordon, J.I.*, et al.* (2010). QIIME allows analysis of high-throughput community sequencing data. Nature methods *7*, 335-336.

Chassaing, B., Koren, O., Carvalho, F.A., Ley, R.E., and Gewirtz, A.T. (2013). AIEC pathobiont instigates chronic colitis in susceptible hosts by altering microbiota composition. Gut.

Darfeuille-Michaud, A., Boudeau, J., Bulois, P., Neut, C., Glasser, A.L., Barnich, N., Bringer, M.A., Swidsinski, A., Beaugerie, L., and Colombel, J.F. (2004). High prevalence of adherent-invasive Escherichia coli associated with ileal mucosa in Crohn's disease. Gastroenterology *127*, 412-421.

Edgar, R.C. (2010). Search and clustering orders of magnitude faster than BLAST. Bioinformatics *26*, 2460-2461.

Edwards, A.D., Diebold, S.S., Slack, E.M., Tomizawa, H., Hemmi, H., Kaisho, T., Akira, S., and Reis e Sousa, C. (2003). Toll-like receptor expression in murine DC subsets: lack of TLR7 expression by CD8 alpha+ DC correlates with unresponsiveness to imidazoquinolines. European journal of immunology *33*, 827-833.

Gulati, A.S., Shanahan, M.T., Arthur, J.C., Grossniklaus, E., von Furstenberg, R.J., Kreuk, L., Henning, S.J., Jobin, C., and Sartor, R.B. (2012). Mouse background strain profoundly influences Paneth cell function and intestinal microbial composition. PloS one *7*, e32403.

Hamady, M., Walker, J.J., Harris, J.K., Gold, N.J., and Knight, R. (2008). Error-correcting barcoded primers for pyrosequencing hundreds of samples in multiplex. Nature methods *5*, 235-237.

Lozupone, C., and Knight, R. (2005). UniFrac: a new phylogenetic method for comparing microbial communities. Applied and environmental microbiology *71*, 8228-8235.

Tibshirani, R., Hastie, T., Narasimhan, B., and Chu, G. (2002). Diagnosis of multiple cancer types by shrunken centroids of gene expression. Proceedings of the National Academy of Sciences of the United States of America *99*, 6567-6572.